

Investigating Bond Wire Resonance in ATLAS

Part II Experimental & Theoretical Physics – Long Vacation Work

Thomas Barber, King's College

This investigation was carried out over the long vacation 2003 in the Particle Physics Dept. of Rutherford Appleton Laboratory, Oxford. I was supervised by Dr William Murray during my time there.

Except where specific reference is made to the work of others, this work is original and has not been already submitted either wholly or in part to satisfy any degree requirement at this or any other university.

Signed -

Date -

Summary

The aim of this report is to gain a better understanding of the nature of bond wire resonance and how they might affect hardware to be used in the semiconductor tracker (SCT) of the ATLAS experiment¹. This effect occurs when bonds carrying current are placed in a magnetic field, giving rise to Lorentz forces. An oscillating current at the resonant frequency of the wire can cause large amplitude mechanical vibrations which weaken and eventually break it. The investigation falls into three main sections:

- Theoretical analytic work predicts that the resonant frequencies depend on the inverse square of the length of the bond wire and are directly proportional to diameter. Also the amplitude of the oscillations depends on the fourth power of length. FEA normal mode simulations confirm this and also show that the orientation of the wire in the field is crucial. Situations where the Lorentz force is out of the plane of the wire loop were found to give larger amplitude oscillations. Wire bonds of the dimensions to be used in ATLAS were predicted to oscillate in the kHz region.² 3mm long bonds were predicted to oscillate at around 12kHz.
- Experiments were then carried out using test bonds to confirm the predictions and classify the resonances. A transient response method, which looked at the back e.m.f. through the wire, was found to be very powerful in locating resonant frequencies. 0.9mm and 2.3mm bonds were found to vibrate at 77 ± 5 kHz and 17.9 ± 0.4 kHz respectively. A combination of the back e.m.f. method and photographic analysis over a range of frequencies gave a Q value of 137 ± 38 for 2.3mm long wires.
- Finally, tests were made on hardware that is to be used in ATLAS. The three wires identified as potentially at risk (i.e. would carry mA signals at kHz frequencies) were the LVDS wires on the barrel opto-package and the K5 forward hybrid. Also tested were the forward opto-package bond wires to the VCSEL chips. No resonant vibrations could be found with the wires in their ATLAS orientations, either due to less dangerous modes being excited or the short wires giving small amplitude oscillations. It is recommended, however, to impose a VETO against constant frequency triggers that may cause damage over a long period of time.

¹ For more information on ATLAS and the SCT visit <http://atlasexperiment.org/>

² Wires used are SiAl bonds with 25um diameter and lengths of 1-3mm

1 - Introduction

Modern particle physics detectors require strong magnetic fields to distinguish charged particles that move through them. Any bond wires used in the experiment to carry an oscillating current will feel a Lorentz force and begin to vibrate. If this Lorentz driving force is at the resonant frequency of the bond wire, the amplitude of oscillations is increased, eventually causing the wire to break under metal fatigue.

This mechanism was identified as the cause of failures in detector readout in the Collider Detector at Fermilab (CDF) experiment in 2002.³ Their solution was to minimize the possibility of constant pulses at resonant frequencies. Another solution was to encapsulate the bond foot in a silicon elastomer, which gave very strong damping. This was not implemented, however, as they have no access to the modules in the experiment.

This report investigates the problem and whether it could occur in ATLAS. Initial studies by Tony Weidberg and Dave Charlton⁴ demonstrated that resonance and breaking of bond wires could be possible with bonds of similar dimensions to those used in ATLAS.

This report divides the problem into three parts. First of all there is a section on the theoretical nature of the resonances, aiming to predict their frequency and relative amplitude via both analytic and simulation methods. Second, studies using test bonds were carried out to confirm the prediction, investigating frequencies and quality value of the oscillations. Finally some tests were done using actual ATLAS hardware, simulating a worst case scenario in terms of currents and signal frequency.

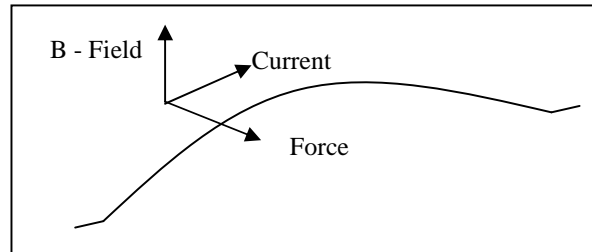


Figure 1.1 – Diagram showing how Lorentz forces arise on bond wires carrying current in a magnetic field.

2 - Bond Wire Resonant Frequency Predictions

The aim of this section is to find out how the variation in bond wire parameters, such as length, diameter and loop height, effect the resonant frequencies. This will hopefully make the resonances much easier to find. The report has two parts, an analytical section looking directly at equations and a section containing the results of finite element analysis (FEA) simulations. Both techniques use normal mode analysis to predict the position of resonant frequencies.

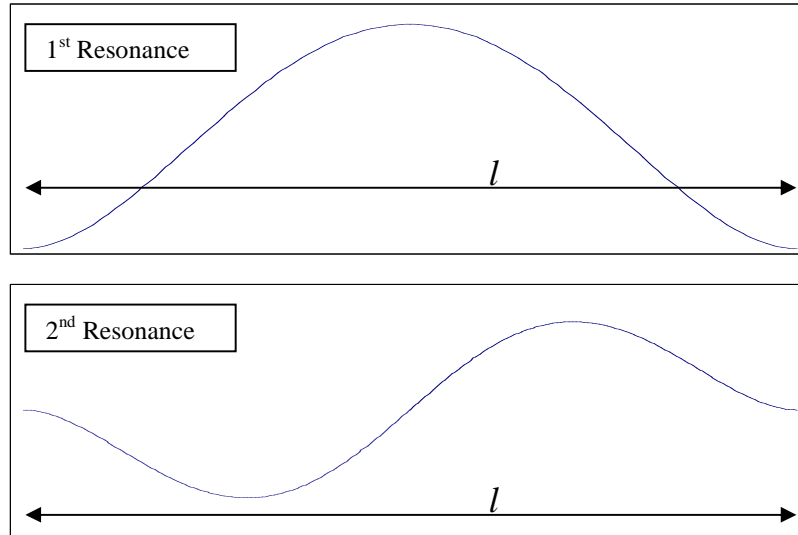
2.1 Analytical Model

In this simple analytical model of a bond wire, consider a straight beam of material, length l , which is clamped at both ends. If the wire were constrained to oscillate in only one dimension, it would be expected that the first two normal modes of oscillation have the form as shown in figure 2.1. For a higher frequency mode, n , there would be $n-1$ nodes, but the shapes would be similar.

³ The full CDF report by Reid Mumford can be found at http://ssd-rd.web.cern.ch/ssd-rd/bond/talks/reid_cdf.pdf

⁴ For more information see the report at http://www-pnp.physics.ox.ac.uk/~weidberg/Resonant_Bond_Wire_Problem.doc

Figure 2.1 – Sketches of first two normal modes.



To find the shape and frequencies of the equations, we can consider the wire as a loaded beam.⁵ It can be shown that the differential equation for the vertical displacement, y , of a beam of length l is:

$$y'''' = \frac{F}{D} \quad (2.1)$$

where F is the force per unit length acting on the bar and D is its flexural rigidity, equal to:

$$D = \frac{EI}{1 - \sigma^2} \quad (2.2)$$

where E is the Young's modulus of the material, I its moment of inertia and σ the Poisson's ratio. Solving the differential equation with boundary conditions for a beam clamped at both ends:

$$\begin{aligned} y(0) &= 0 \\ y'(0) &= 0 \\ y(l) &= 0 \\ y'(l) &= 0 \end{aligned} \quad (2.3)$$

gives the solution of:

$$y = \frac{F(l-x)^2 x^2}{24D} \quad (2.4)$$

This is the shape of the first normal mode as sketched above. To find the frequency of oscillation, consider the maximum displacement, which will occur at $x=l/2$ and has a value of:

$$y = \frac{Fl^4}{384D}$$

(2.5)

This is an interesting equation because for a given force, the magnitude of displacement varies with the forth power of length. In a practical context, oscillations of longer wires will have larger amplitudes and will be much easier to see with a camera. For example a 3mm wire will be displaced 81 times further than a 1mm wire. Rearranging this equation (2.5) gives the restoring force per unit length for a given vertical displacement. Equating this with the subsequent acceleration yields the equation for simple harmonic motion.

$$\ddot{y} + \frac{384D}{\rho A l^4} y = 0$$

(2.6)

where A is the cross sectional area of the wire and ρ is the density. For a wire of circular cross sectional area and diameter d and substituting a value of $I = \pi d^4/64$ for the moment of area gives a frequency of oscillation of:

$$\omega = \frac{d}{l^2} \sqrt{\frac{24E}{\rho(1-\sigma^2)}}$$

(2.7)

For the second normal mode there is a similar dependence on length and diameter, but the term inside the square root is slightly different.

2.2 - Simulations

An number of bond wires were constructed using the JL Analyser FEA package.⁶ The parameters used for constructing these models where the bond length, diameter and the loop height. A simple quadratic curve was fitted to these variables to give an estimation of the bond shape, with a 0.1mm foot length at either end. The model was then meshed as a circular beam and given the following properties consistent with wire bonds for ATLAS:

Young's Modulus	69Gpa
Density	2710 kgm-3
Poisson's Ratio	0.330

A side view of the bond model is shown in figure 2.2.

Figure 2.2 – Simulation Model



⁵ See Eric Weisstein's World of Physics for more information at <http://scienceworld.wolfram.com/physics/beam.html>

⁶ See www.autofea.com for program details.

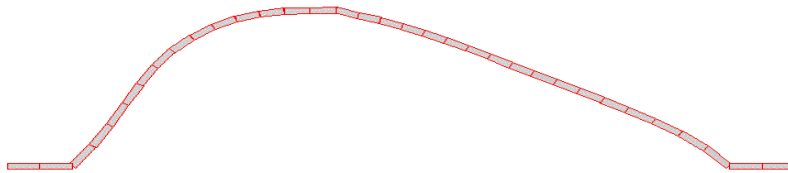
To mimic attachment to the bond pad, restrictions in all degrees of freedom were imposed on both of the bond feet. Frequency analysis was performed on a number of bonds to find the frequencies of the normal modes. The shapes of the first five modes are shown in figure 2.3.

Figure 2.3 - Shapes of the Normal Modes

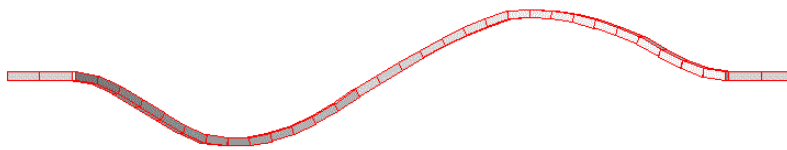
Mode 1 – Top View



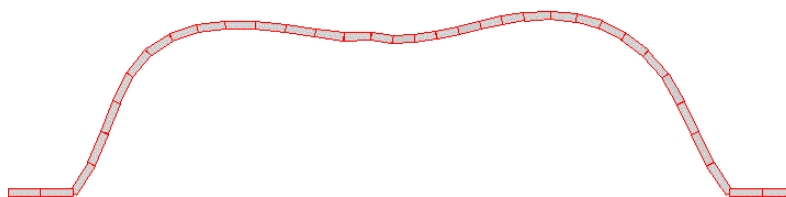
Mode 2 – Side View



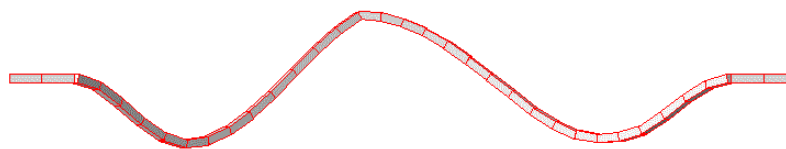
Mode 3 – Top View



Mode 4 – Side View



Mode 5 – Top View



The shapes of the odd numbered modes are those predicted using the beam model earlier. (compare with figure 2.1) The even numbered modes correspond to displacements in the plane of the wire. As there will be Lorentz forces in both directions due to the different orientations of hardware in the ATLAS B-field, both types will be considered.

The simulations showed the normal mode frequencies have an inverse square relationship with bond length and direct proportionality with bond diameter. This backs up the earlier predictions made with the beam model. Plots of the frequency dependence on length and diameter are shown in figures 2.4 & 2.5 respectively.

Figure 2.4 – Dependence of Frequency on Length

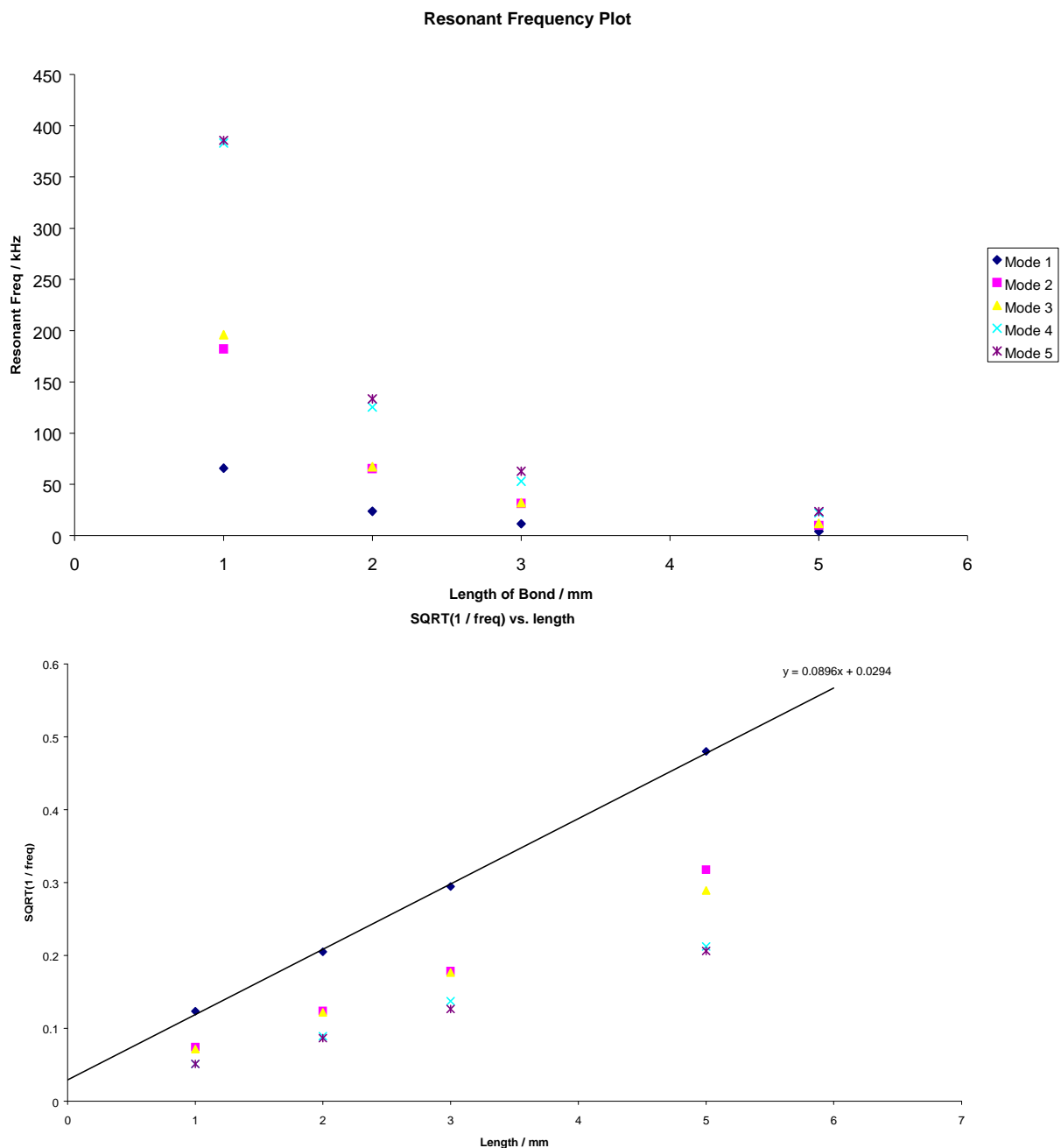
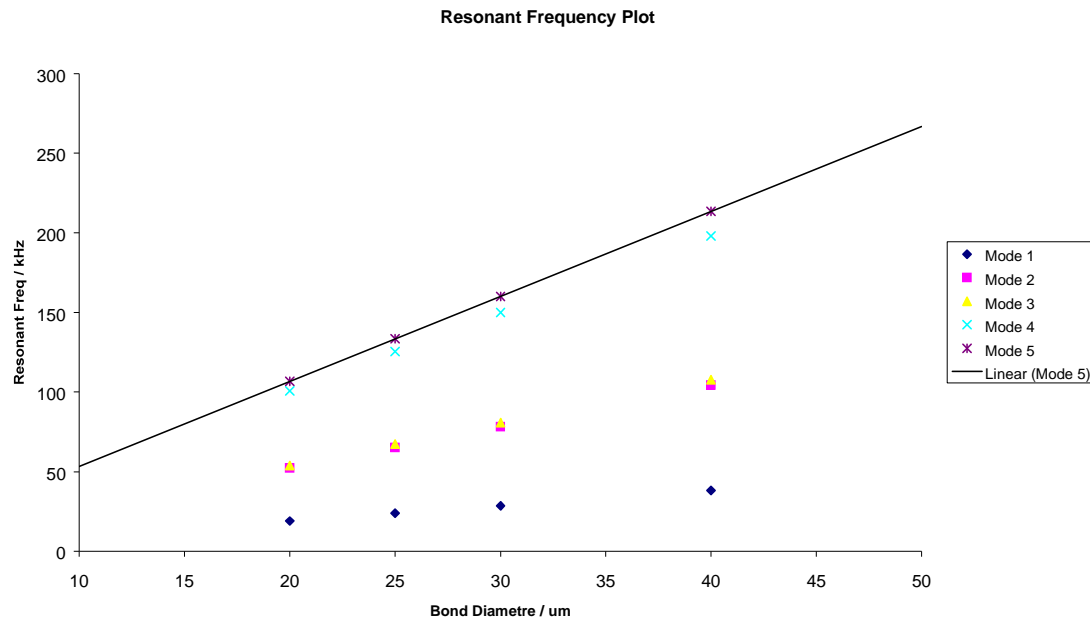
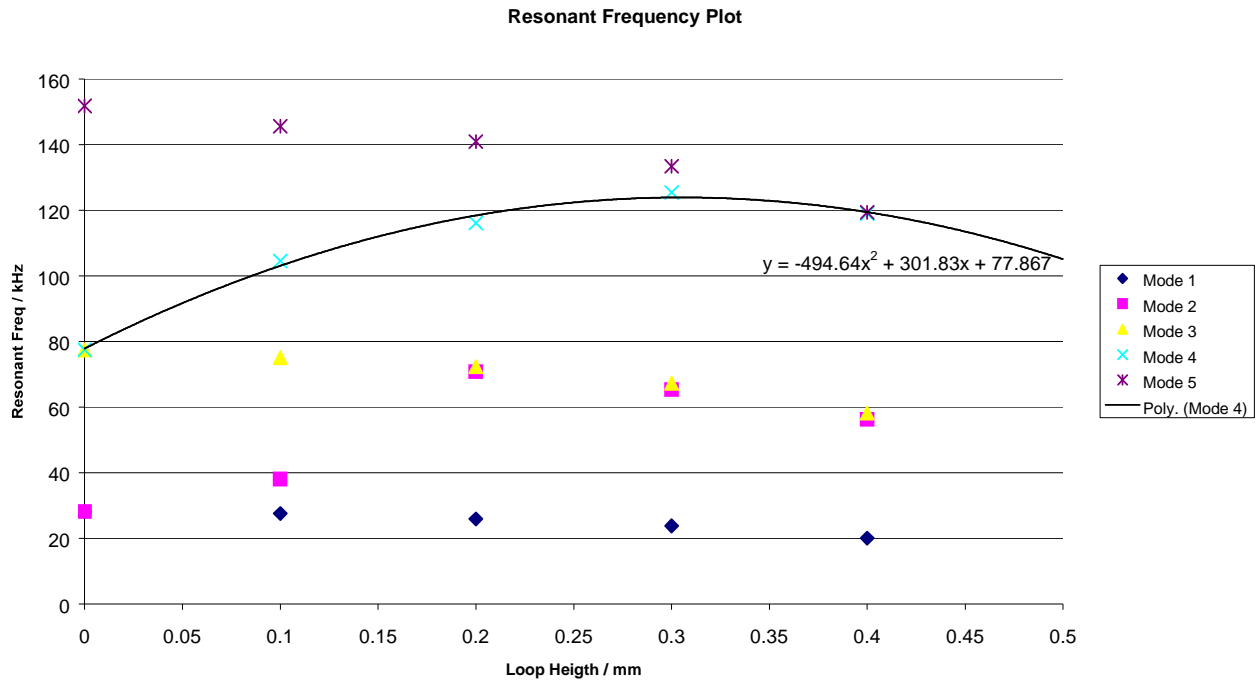


Figure 2.5 – Dependence of Frequency on Diameter



The dependence on bond loop height is slightly harder to explain precisely and may depend on the exact shape of the bond wires which is not, in reality, quadratic. Importantly there is only a small change in the fundamental frequency ($\sim 9\%$) for loop heights between 0.2mm and 0.3mm, which are the heights expected in the opto-package bonds in ATLAS (see section 5). A plot of the frequency dependence on loop height is shown in figure 2.6. There are some interesting points to make; at zero loop height degeneracy occurs and there are two modes for each frequency. This is because the bond is just a straight wire and is free to oscillate in two dimensions. (Although this will not happen in reality.) All of the points seem to fit a quadratic curve, although this may be due to the idealized shape of the bonds. The exception to this is mode two for which there is a jump between frequencies at 0.1mm and 0.2mm. Another interesting point is that as the loop height gets larger degeneracy seems to be occurring again, but with different modes. This may be because as the dimensions become more extreme, the modes in different directions become indistinguishable from each other.

Figure 2.6 – Dependence of Frequency on Loop Height



2.3 - ANSYS Simulations

Some simulations were carried out with ANSYS, a more advanced FEA package, using a more realistic bond wire, with $l=2.6\text{mm}$ and $h = 1.4\text{mm}$. This showed the same shapes of normal modes as before, with a fundamental frequency at 13.5kHz. A spectrum analysis could also be performed using a sinusoidal Lorentz driving force of $5.2\text{e-}5\text{N}^7$. The forces were applied in both the Y and Z directions to simulate the possible orientations in the magnetic field in ATLAS. The responses are shown in figures 2.7 & 2.8.

These show that the Y & Z direction forces will excite the even and odd numbered modes respectively. Also looking at the scales of both plots shows that the Y direction amplitude is roughly two orders of magnitude smaller than that for the Z. In the Y direction case the amplitude is an order of magnitude less than the diameter of a bond wire, so will probably not be a problem in ATLAS. The fundamental of the Z direction response shows a much larger magnitude of 0.72mm, which would be large enough to be seen and likely to cause problems. This corresponds to the 1st normal mode of figure 2.3 above. The other harmonics on the Z diagram are only ~5% of the amplitude of the fundamental, but may still be detectable as they correspond to amplitudes of ~1.6 bond diameters.

⁷ Calculated from a 20mA current, 2T field and 2.6mm of wire, using $F = BI l$

Figure 2.7 – Frequency Response in the Y direction.

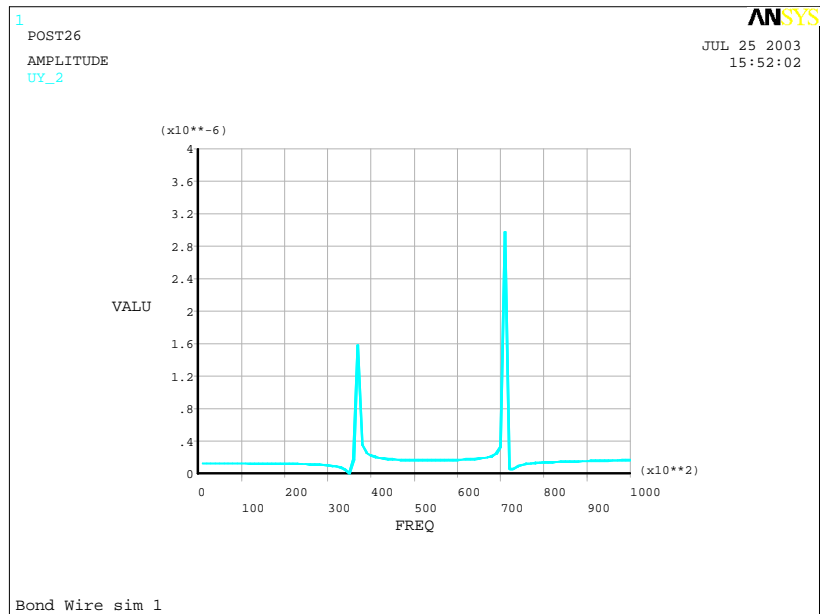
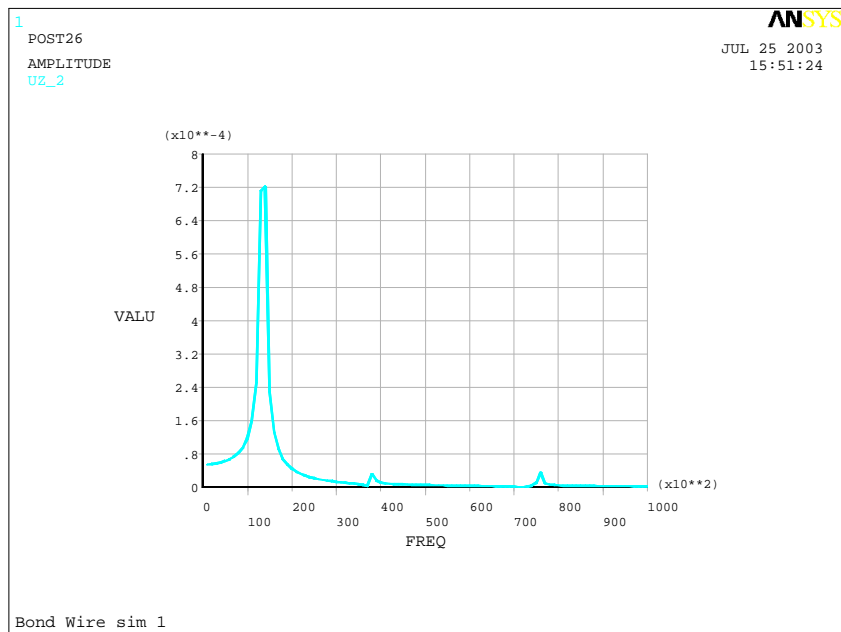


Figure 2.8 – Frequency Response in the Z direction



2.4 – Summary of Predictions

The main conclusions from this are the dependence of frequency on length is an inverse square relationship and there is a direct proportionality with diameter. In reality diameter will be fairly constant compared to length variation.

$$f \propto \frac{d}{l^2} \quad (2.8)$$

Also the amplitude of oscillations will depend on the fourth power of length, making shorter bonds less likely to break as a result of resonance.

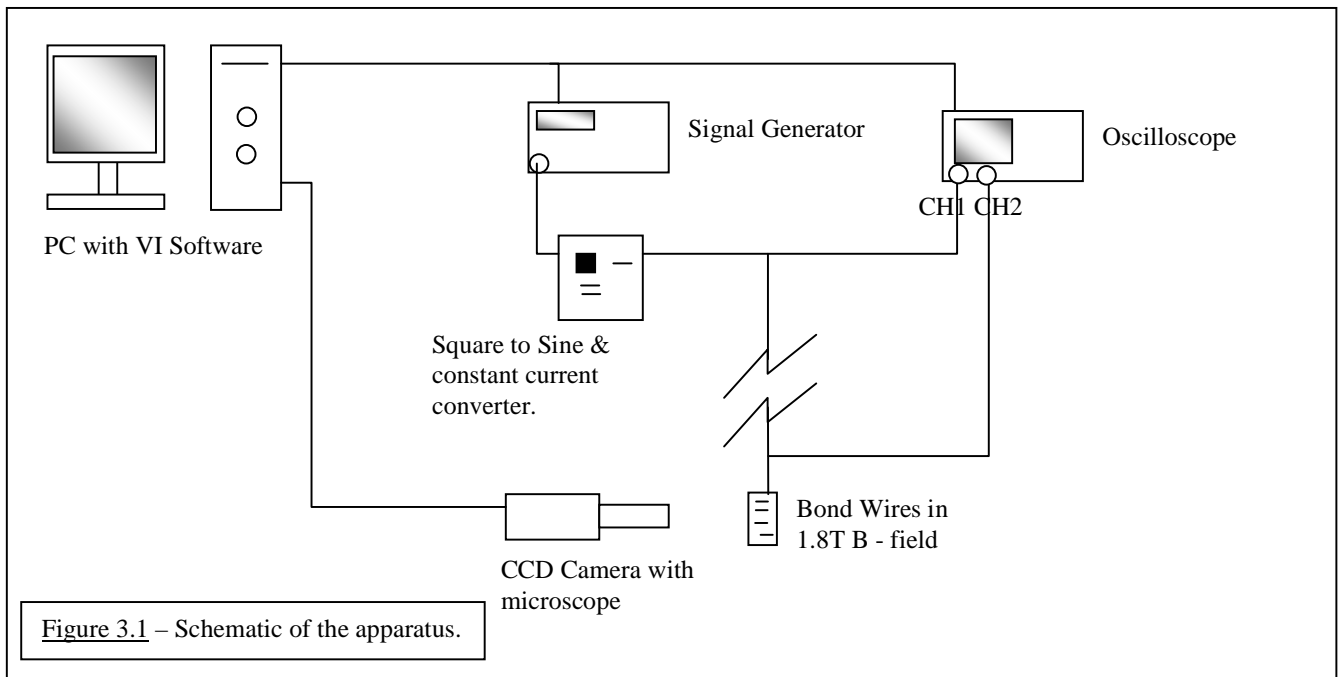
$$A \propto l^4 \quad (2.9)$$

The loop height variation is harder to quantify, but empirical curves could be fitted to determine the variation in frequency due to uncertainty in height.

Also it seems that the more dangerous modes occur when the B-field is in the plane of the loop, (odd numbered modes) producing forces in the Z direction. In this case the fundamental poses the largest threat, with possible danger from harmonics. The even modes may not be detectable and hence unlikely to cause problems in ATLAS.

Section 3 – Experimental Method

To investigate the resonant frequencies of these bond wires a number of techniques were suggested. The most direct way was to simply monitor the bond wires with a video camera with microscope attachment and scan a frequency range to try and see the oscillations. As most video cameras have a refresh rate of only 75Hz compared to 10-20kHz expected for the bond oscillations, the resonating wire would appear to widen as it oscillates.



Another possibility was to look at the transient response of the bond wires. In practice this means feeding a low frequency pulse through the wires and looking at the voltage response. The initial pulse will cause the wire to be displaced from equilibrium and, as the signal contains Fourier components at all frequencies, will make it oscillate at its resonant frequency when released. The wire will then be moving in a magnetic field, generating a back e.m.f. across the wire which can be measured on an oscilloscope.

To drive the wires a standard square wave generator was used connected to a custom built square to sine circuit board and a Howland constant current source, with a range up to around 40mA. (see appendix) The voltage was measured in two places – at the output of the sine signal and closer to the field across the bond wires. The CCD camera was linked to a video capture PC card. Both the signal generator and the scope were controlled by the PC using a GPIB interface. (See figure 3.1 for schematic.) A virtual instrument (VI) program was written in Labview to scan a frequency range whilst taking snapshots with the camera and recording voltages across the wires. Figure 3.2 shows the basic program structure whilst the entire program is shown in the appendix in section 8.1.

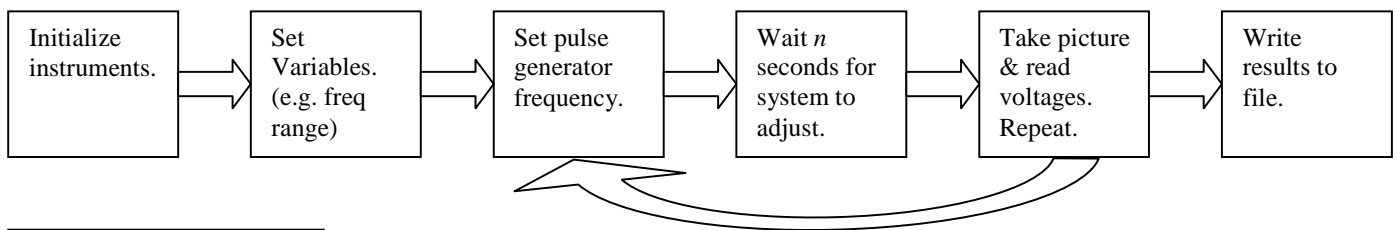


Figure 3.2 – VI flowchart.

To look at the transient response the signal generator was set manually to give a low frequency 1V pulse of 1ms duration. The signal across the bond was monitored using the scope and averaged over a number of sweeps (1000 or 4000) to give a clean signal and reduce errors. A fast Fourier transform (FFT) was then performed of this to identify any oscillating signals in the power spectrum.

The magnet used in the experiment was a 1.8 T electromagnet, close in field strength to that of ATLAS, which will be at 2T.

Two different lengths of test bonds were used, (0.9mm and 2.3mm) laid down onto gold tracks. A set of overbonded wires of 2.3mm were also investigated for comparison (section 4). As well as this, the actual ATLAS components at risk were investigated (section 5). All the bonds tested were standard 25um, 99% Al, 1% Si wires.

Section 4 – Test Bond Results

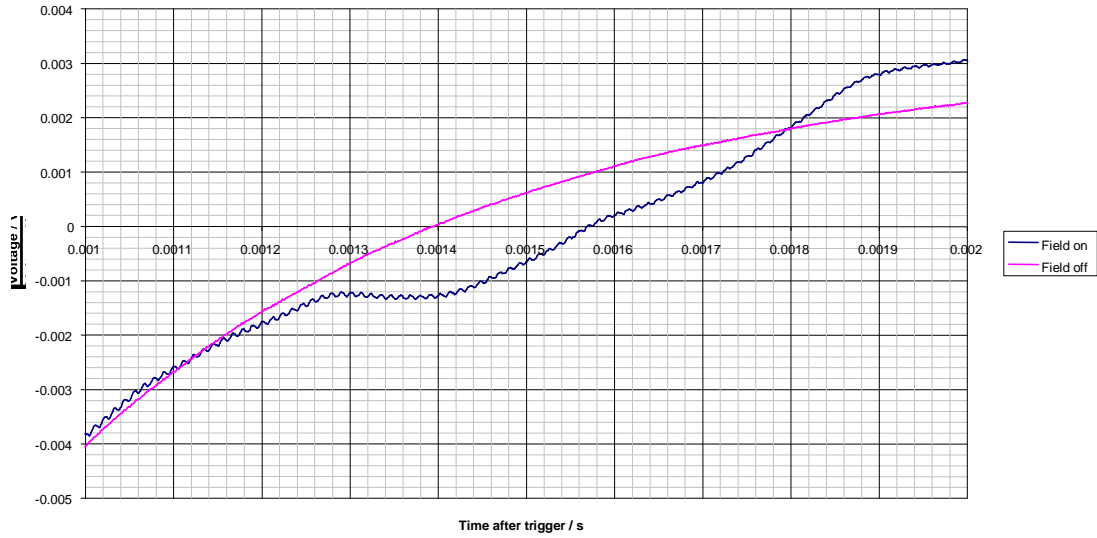
4.1 - Short Test Bonds – 0.9mm

The first set of experiments uses test bond wires to help classify the general nature of the oscillations and resonant frequencies. Short wires were used to begin with but despite extensive investigation with the camera of the wires, nothing was seen. This may be because the amplitude of the oscillations is too small to be seen, and longer wires may give visible results.

The transient method did however yield some interesting results. A 1ms long pulse was used with 50ms period, monitoring the voltage across the wire around 1ms after the falling edge of the pulse. The response of the system with and without the field is shown in figure 4.1, averaged over 1000 sweeps. The response shown is from track 4 on the test board. (The “track” quoted throughout section 4 is simply an arbitrary experiment number.)

Figure 4.1

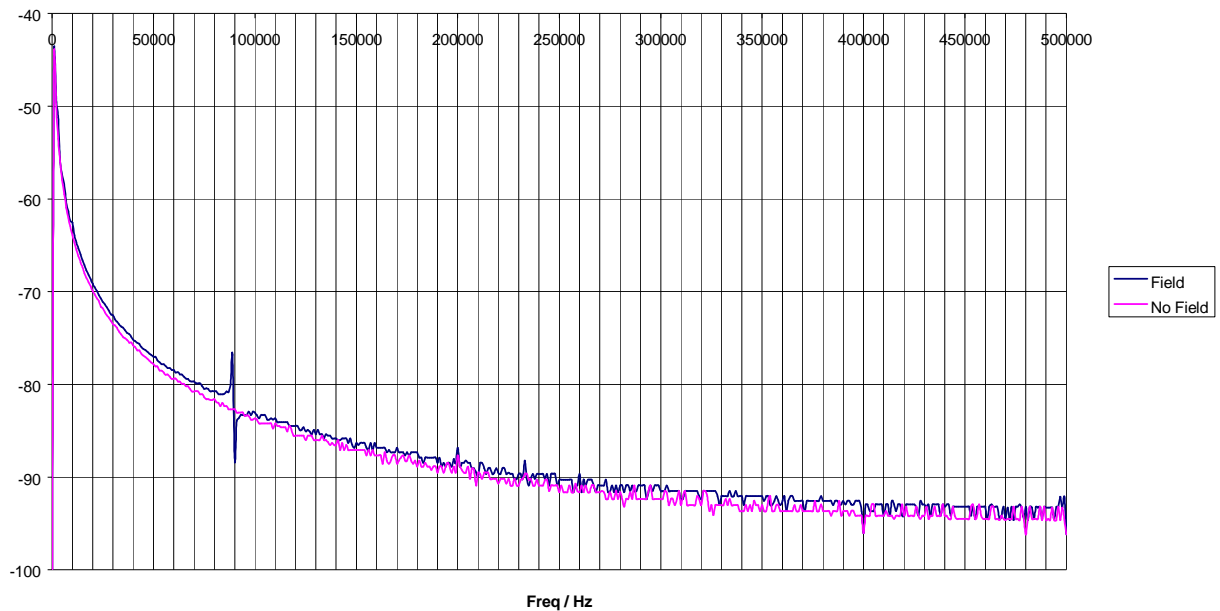
Transient Response of the System



With the field on there appears to be a high frequency oscillation superimposed onto a lower frequency signal ($\sim 1\text{kHz}$). This low frequency is unlikely to be bond wire oscillations, but could be due to other components of the board reacting to the magnetic field. The most likely candidates are the wires used to connect the signal cable to the actual bonds. From the simulations, a signal in the 1kHz range could be caused by a 5cm length of copper wire, of comparable to the lengths of actual wires used. The higher frequency signal is likely to be a bond wire oscillating. An FFT of the two signals is shown in figure 4.2.

Figure 4.2

Frequency Response Power Spectrum



There is a clear peak in the FFT which does not appear with the field switched off. The peak also shifts from positive to negative at its highest point, implying a phase change across this region. The peak occurs at $89.5 \pm 0.5\text{kHz}$ which is consistent with a bond wire with a length of 0.85mm and a loop height of 0.3mm.

To investigate this further, the wire above and three others were tested in the field but this time averaged over 4000 sweeps to decrease errors. Four wires were tested and their frequencies are shown in figure 4.3. In two cases the negative side of the peak was not seen; this may be because the resonance is too narrow for the FFT resolution so only the positive peak is displayed. There was a significant variation in amplitudes of the peaks compared to the surrounding level. Visual inspection of the wires after the experiment revealed that the smaller amplitude wire had been distorted which could be the cause.

Figure 4.3 – Resonance Peaks for Short Wires

Track Number	Frequency / kHz	Amplitude / dB
3	74	5.1
4	90	5.8
5	75	2.7
6	69	12.2
Mean:	77	6.5
Std. Dev:	9	4.0

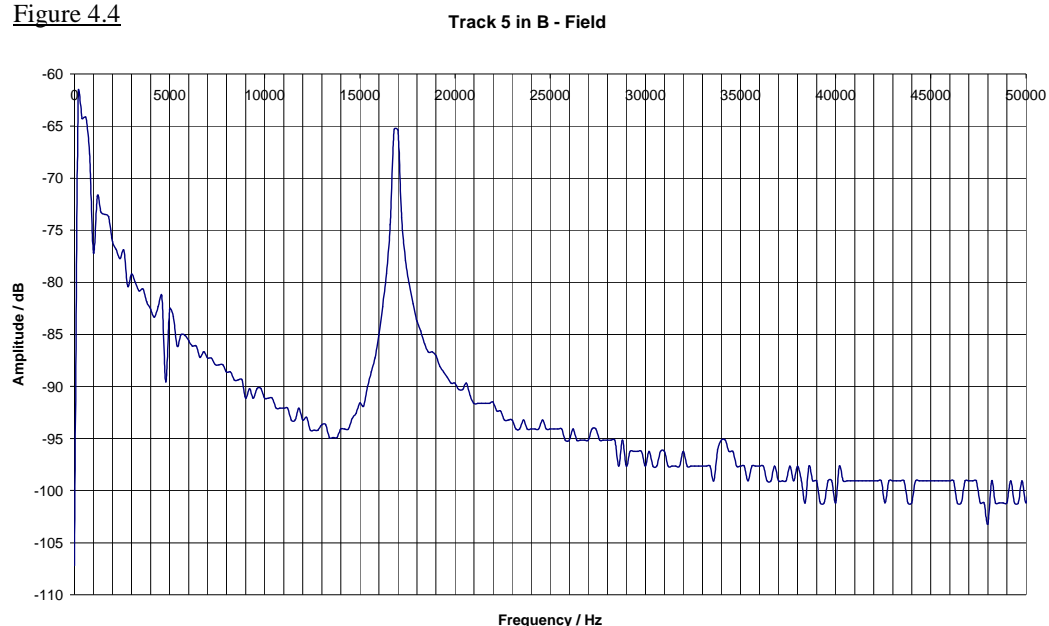
The standard deviation corresponds to a frequency variation of ~12%, giving a length variation of 6%. Assuming all of this error comes from the placement of two bond feet at each end of the wire, the accuracy of the bonding machine would be ~ 27µm.

An FFT of the voltage with no bond wire, (i.e. a shorted track) showed no peak in the spectrum, but still contained the low frequency resonance, implying it is not a bond wire effect. Also changing the orientation in the field to give a force in the plane of the wire loop also showed no peak. This is expected as a different set of modes are excited by this orientation of field, with much lower amplitudes. (see section 2.3) It would therefore be expected that the peaks moved and were smaller. In reality they were probably lost in the background noise.

4.2 - Long Test Bonds – 2.3mm

Longer bonds were also tested to try and obtain visual confirmation of the resonance. The back e.m.f method was used to locate the approximate position of the resonant frequencies before trying to view them directly. As expected these bonds show lower resonant frequencies with much larger amplitudes due to their length. An example of the back e.m.f. FFT for one of the bonds is shown in figure 4.4.

Figure 4.4



The resonant frequency is now much clearer at 17.0 ± 0.2 kHz and there is a hint of a first harmonic at 34.6 ± 0.2 kHz. The resonant frequencies of four wires were measured using this method and are summarized in the table below: (figure 4.5)

Figure 4.5

Bond Track	Frequency / kHz
5	17.0
6	17.8
7	18.6
8	18.0
Mean:	17.9
St. Dev:	0.7

The FEA prediction for a bond wire of 2.3mm and a 0.3mm loop height is 18.0 kHz, and so is in very good agreement. Once again, the mean and standard deviation correspond to a bond foot placement error of 22µm.

The bond wire on track 7 was scanned with a constant current sine wave of 10mA from 15kHz to 20kHz and the wire width appeared to increase as it reached resonance. Closer to the resonant frequency the wire is clearly oscillating, as the extremes of movement appear bright with a dark area between. The largest amplitude of oscillations occurred at 17.4 kHz, which is significantly lower than predicted by the back e.m.f. method. This may be because the system is not linear and the low frequency components in the pulse may affect the bond wire resonance. Photos of the oscillating bonds are shown in figure 4.6.

When trying to scan other bonds with sinusoidal currents the resonance seemed to disappear. After showing a clear peak with the e.m.f. method and initial oscillations close to resonance a scan over the frequencies showed no difference in width. Returning to the e.m.f. method revealed the peak had disappeared. This happened with the three remaining bonds and the cause is still unknown. It is possible that initial fatigue due to driving at resonance or close to it for a short time may prevent oscillations occurring. The wires may have warmed making them more malleable or cracks may prevent oscillation. It would be interesting to do further tests to see if resonance recurs after the bonds have rested.

Figure 4.6 – Bond Wire Photos

15.0 kHz – Away From Resonance



17.2 kHz – Approaching Resonance



17.4 kHz – At Resonance



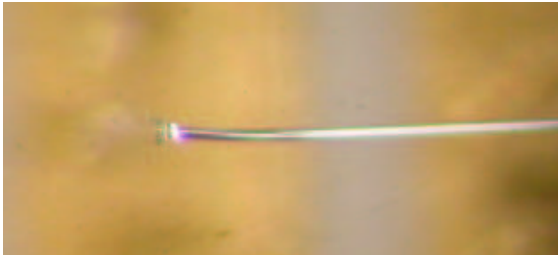


Figure 4.8 – Overbonded wire after breaking.

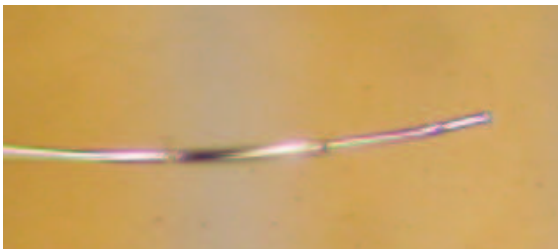


Figure 4.9 – Normal bond wire after breaking.

4.3 - Overbonding Effects

Some overbonded wires were made with the same length as before (2.29mm) to investigate any effects this causes. Overbonded wires occur when too much power or pressure is put into the bonding wedge causing the foot width to increase beyond an optimum value (around 1.2 times wire diameter). This means that the heel of the bond is weakened and may be more prone to damage when driven at resonance. (reference to Jeff's report?) The overbonded wires show similar resonant frequencies when tested with the back e.m.f. method, as shown in figure 4.7.

Figure 4.7 – Resonant Frequencies of Overbonded Wires

Bond Track	Frequency / kHz
1	17.4
2	13.8
3	17.3
Mean:	16.2
St. Dev:	2.1

The wire across track 2 also showed a large peak at around 25.8 kHz, which seems too low to be a harmonic. To investigate this further the wire was run at 12 kHz with a 10mA sinusoid. It could be seen oscillating for a few seconds before dramatically breaking off. A photograph of the fracture is shown in figure 4.8. Unfortunately, after this, the same problem occurred as with the optimal wires and the resonances seemed to disappear in the remaining wires. The well-bonded wires are understood to break on a time scale of minutes rather than seconds after being driven at their resonant frequency⁸. After inspection of the board after testing it was found that one of the optimal wires had also broken. Whether this was due to fatigue at resonance or fusing due to high currents is not known. A photo of the wire is shown in figure 4.9.

4.4 - Q – Factors

The quality factor of an oscillation (Q – factor) is defined by:

$$Q = \omega \frac{\langle U \rangle}{\langle P \rangle} \quad (4.1)$$

where ω is the angular frequency, $\langle U \rangle$ is the average energy stored per cycle, $\langle P \rangle$ is the average power dissipated per cycle. A high Q factor indicates a long decay time, low damping and narrow resonant peak, whereas small Q factor gives a broader peak and short decay time.

The Q factor for the resonances of the 2.3mm bonds can be evaluated by three different methods.

4.4.1 - Transient Curve Fitting

⁸ For more information see the CDF report.

The transient responses of the track 3 (overbonded) and 5 (normal) bonds as measured using the back e.m.f. method were fitted to a series of three decaying sinusoidal oscillations (corresponding to damped SHM solutions) of the form:

$$A = A_0 \exp(-\gamma_0 t) \sin(\omega_0 t + \phi_0) + A_1 \exp(-\gamma_1 t) \sin(\omega_1 t + \phi_1) + \dots$$

(4.2)

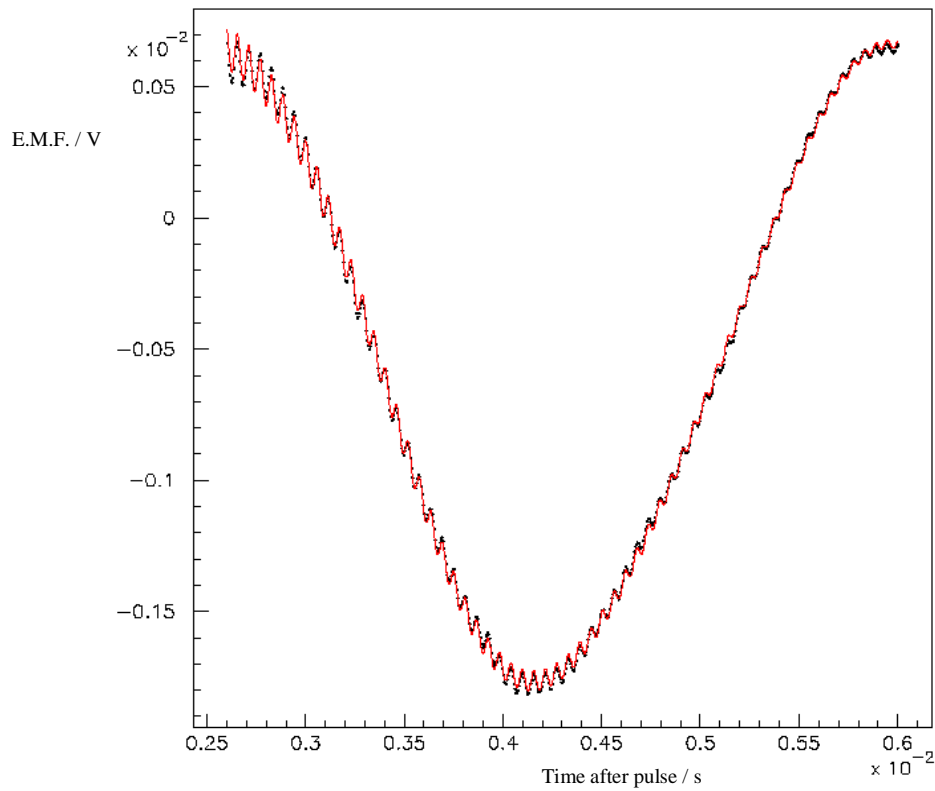


Figure 4.10 – The Transient Response of track 5 with fitted curve shown as solid line. The fit picks out two low frequency components and one at higher frequency.

A plot of the fit is shown in figure 4.10. The fit shows some low frequency components at around 1kHz, probably due to other wires in the system, and a higher frequency component at around 17kHz, due to the bond wire. The Q value in this case can be derived as follows:

$$Q = \frac{\omega_0}{2\gamma}$$

(4.3)

A summary of the high frequency components' properties are shown in figure 4.11. Both of the frequencies agree with the previous measurements from the FFT peaks within experimental error.

Figure 4.11 - High Frequency Properties

Track	Frequency / kHz	Gamma / Hz	Quality Factor
3 – Overbonded	16.9±1.6	46.6±4.4	181±25
5 – Normal	17.3±0.4	77.2±1.9	112±4

4.4.2 - FFT Peak Bandwidth

The Q - factor can also be given by:

$$Q = \frac{\omega_0}{\Delta\omega} \quad (4.4)$$

where ω_0 is the resonant frequency and $\Delta\omega$ is the full width half maximum (FWHM) of the peak in the power spectrum. This can be evaluated from the FFT curves obtained from the back e.m.f. method. A summary of the results is shown in figure 4.12. All frequency errors are $\pm 50\text{Hz}$ and the mean and standard deviation are shown for the overbonded and normal tracks.

Figure 4.12

Track	Frequency f_0 / kHz	Bandwidth Δf / Hz	Q Factor
1	17.37	250	69±14
2	13.81	200	69±18
3	17.30	340	51±8
		Mean:	63
		St. Dev:	10
5	16.90	320	56±9
6	17.76	270	65±12
7	18.60	150	124±41
8	17.99	190	95±25
		Mean:	85
		St. Dev:	40

From this there is some indication that normally bonded wires may have a higher quality factor but the two values for the means are in agreement. The values for tracks 5 & 3 are both smaller than the curve fitting method. This may be due to the resolution of the FFT which only has points every 200Hz. This may make the exact magnitude and frequency of the peak ambiguous. Looking at the FFTs for tracks 7 & 8 which have much higher Q factors, actual data points occur close to the peak, whereas the others have points either side.

4.4.3 - Lorentzian Curve Fitting

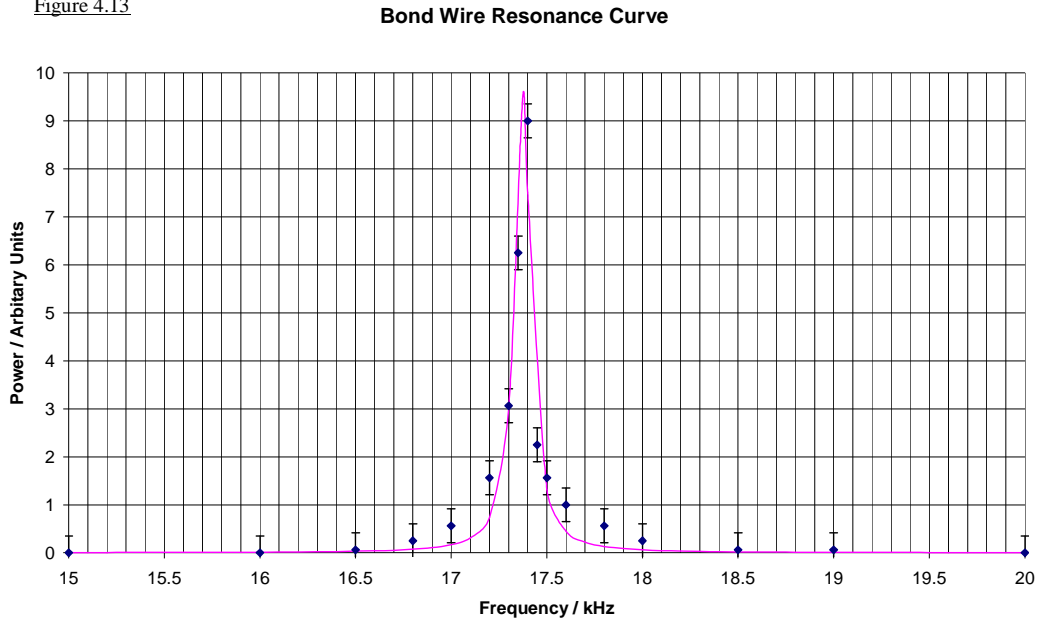
Photo analysis of track 7 at frequencies close to resonance gives an estimate of the actual amplitude of the oscillating wires. The square of this amplitude gives a value proportional to the power spectrum of oscillations that can be fitted to the Lorentzian peak predicted from driven SHM solutions:

$$P = \frac{H}{4\left(\frac{\omega - \omega_0}{W}\right)^2 + 1} \quad (4.5)$$

where H is the peak height, ω_0 the resonant frequency, W the FWHM of the peak. The best fit gives values of $f_0 = 17.4\text{ kHz}$, $\Delta f = 100\text{Hz}$ and so $Q = 172 \pm 43$. This is in agreement with the FFT method in the previous section for track 7. The Plot of the data points and the fitted curve are shown in figure 4.13 and indicate a good fit at frequencies close to and far from resonance, but seems to underestimate between the

two extremes. This may indicate that there may be other factors in the system not accounted for by the Lorentzian.

Figure 4.13



In conclusion, the quality factor of the oscillations is 137 ± 38 from a combination of methods and bond wires. All but tracks 7 & 8 have been ignored from the FFT peak method. At this precision there seems to be no difference between over-bonded and normal wires.

Section 5 - ATLAS Hardware

Having investigated the phenomenon of bond wire resonance in test bond wires, more specific tests were done on pieces of ATLAS hardware that could be at risk from resonance. This includes any bond wires that could carry signals at constant frequency with high enough current to excite the bonds.

The wires thought to be most vulnerable are those to the opto packages that convert electrical signals into fibre optic light pulses. The barrel opto package (mounted on a kapton dogleg) wires occur with the field perpendicular to the wire loop ("barrel" mode), so will excite the even modes as in section 2.2, which are likely to have very small amplitude. The forward opto packages (mounted onto the forward hybrids) have bonds with the field in the plane of the wire loop, so excite the more the dangerous odd modes ("forward" mode).

Investigations done by Tony Weidberg and Peter Phillips at RAL revealed another area of concern with bond wires from the ATLAS module hybrid to the ABCD chips themselves. A potential problem with the VDD (digital voltage power line) revealed the voltage spike (after an L1 trigger) expected gave a small enough current (0.3mA) not to be a problem. Another problem was mentioned involving the LVDS signal (4mA) carrying the chip data. It may be possible to get a signal that gives a combination of 1's and 0's corresponding to the resonant frequency of the wire. Although unlikely, this is still a possibility and was investigated in the LVDS lines from the forward hybrid VDC chip.

Figure 5.1 shows a diagram of the ATLAS inner detector, marked with the positions of hardware tested.

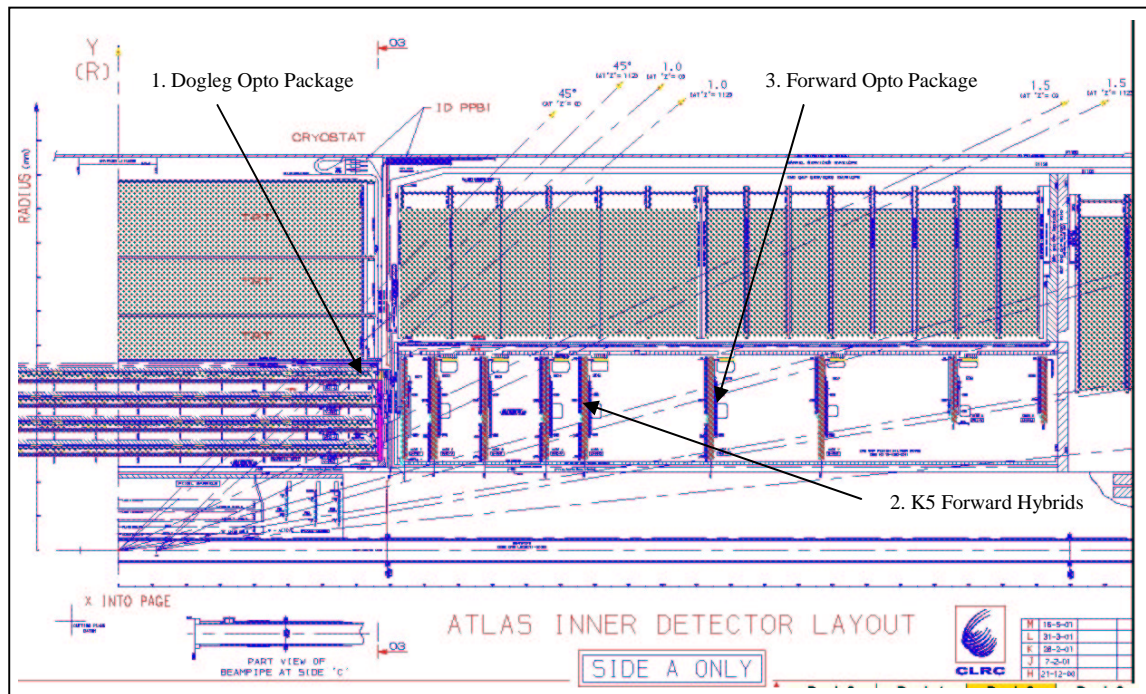


Figure 5.1 – Schematic of the inner detector showing the positions of hardware threatened by the resonant bond wire problem. The forward hybrids and opto package occur around each of the forward discs. There are also doglegs with opto packages along the length of each SCT barrel.

5.1 - Barrel Opto-Package

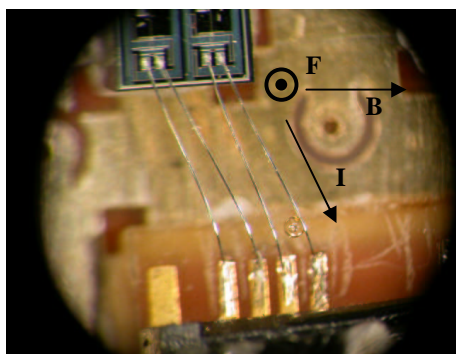


Figure 5.2 – Photo showing the forces on the barrel opto bonds as they are oriented in ATLAS. The VDC chip is shown at the top of the picture, with the VCSEL at the bottom.

The bonds that carry analogue output signals from the VDC chip to the VCSEL chip on the barrel opto packages were monitored with the camera and scanned over a frequency range from 16 kHz to 20 kHz with a 10mA square wave, to simulate a worst case ATLAS scenario. Both the “forward” and “barrel” orientations of field were tested although in ATLAS only the “barrel” case will occur. As the current through the bonds is controlled by a chip it was not possible to monitor the voltage across them directly and so the back e.m.f. method could not be used.

In “forward” mode two sets of resonant frequencies were found for each wire, a fundamental frequency, f , and a resonance at $f/3$. The lower frequency square wave will contain a Fourier component at the fundamental and hence should excite it with lower amplitude. The fundamental frequencies of the two wires were 17.2 kHz and 18.0 kHz (± 0.1 kHz). This is slightly higher than predicted by simulations which predicts 13.2 kHz to 14.0 kHz corresponding to the length range of 2.74mm to 2.65mm with a loop height of 0.3mm. The loop height variation may be responsible for this discrepancy.

In “barrel” mode no resonance could be seen up to 50 kHz despite a predicted a resonant frequency between 33 kHz and 36 kHz. Despite poor picture quality, oscillations of more than one bond wire diameter were not observed, so are unlikely to cause problems in ATLAS.

5.2 - Forward Opto-Package

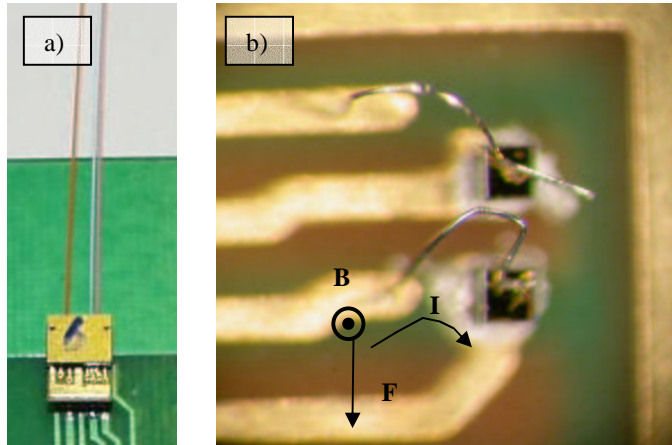


Figure 5.3 Forward Opto-Package photographs. a) shows the overall package with the wires out of view. b) shows the bond wires from the gold tracks to the VCSEL chips.

The two bond wires to the VCSEL chips are in the “forward” orientation but are fairly short ($< 1\text{mm}$) so will have high frequency, low amplitude oscillations. The wires were driven directly through a resistor to give 25mA. Only 10mA is expected in normal ATLAS operating conditions.

The back e.m.f. method showed no peaks up to a frequency of 500 kHz. This puts an upper limit on resonant peaks at 4uV compared to the 80uV peak for the 2.3mm bonds. Visual scans up to 150 kHz revealed no oscillations with amplitude greater than about $\frac{1}{4}$ of a bond wire diameter. Four wires were tested in total.

The wires are estimated to be 0.67mm long with a 0.21mm loop height. Predictions from simulations give an extrapolated fundamental at $131 \pm 11\text{kHz}$. This is encouraging as there are unlikely to be triggers sent at above 100 kHz so any resonances above this will only be hit with higher frequency, lower amplitude Fourier components. This, combined with the low amplitude resonance, indicates that these bonds are unlikely to be at risk.

5.4 - K5 – Forward Hybrid

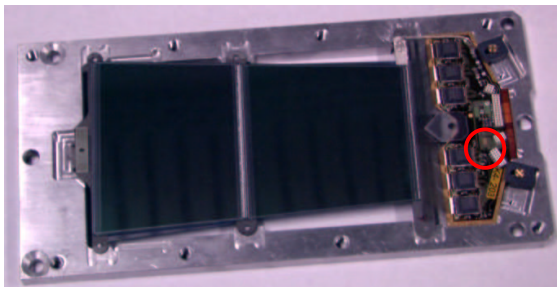


Figure 5.4 – Forward module with hybrid attached. The bonds concerned are in the area circled, carrying LVDS signal from a VDC chip. N.B. Hybrid shown is a K4 version, whereas the version tested is the latest, the K5. The bond lengths on the VDC chip differ significantly between the two.

Similar methods were used to investigate the LVDS bonds from the VDC chip on the K5 forward hybrid.

The back e.m.f. method revealed no resonances of more than 4uV up to 500kHz. Visual scans were made of four different wires and also showed no resonance in the region between 50 kHz and 150 kHz. A typical ATLAS 10mA square wave current was used to pulse the wires.

The wires are $\sim 0.7\text{mm}$ long which predicts a resonant frequency of $118 \pm 10\text{kHz}$. Their short length also means a low amplitude – around 100 times smaller than the 2.3mm test bonds due to the fourth

power relationship. As the largest amplitude seen with the long wires was ~ 16 wire diameters, the largest corresponding amplitude for the K5 bonds is less than 0.2 diameters. As the bond wire showed up as 4 pixels wide on the CCD image, it is not surprising nothing was seen. On this scale it would be very hard to locate the exact resonant frequencies to test the bond wire durability. Prolonged exposure to low amplitude resonant pulse may still, however, be enough to break the bonds by metal fatigue.

5.5 – Summary

From these results it seems that none of the wires tested exhibit the problem of bond wire resonance due to either their orientation in the field or their length. Despite this, the effects of low amplitude, long term fatigue are not known, so imposing some counter measures may be needed as a safety net. As much of the ATLAS hardware has been constructed, encapsulation of the bond feet seems impractical. The best solution is probably to impose a VETO against constant frequency triggers to ensure no wires are driven close to resonance.

At the start of LHC operation, there may be occasions when ATLAS is run at 11kHz. (The machine's revolution frequency) Of the bonds considered, the lowest frequency expected is around 33kHz and this is a low amplitude, even numbered mode. The odd modes expected occur above 100kHz, an order of magnitude higher. If there was a veto imposed on fixed frequencies above 15kHz, all bonds shorter than 2.6mm should be safeguarded.

Section 6 – Conclusions

The main conclusions of this report are as follows:

- Simulations shown that the frequency of bond wire normal modes depends on the inverse square of length and is directly proportional to wire diameter.
- Simplified bond profiles give a resonant frequency of $\sim 12\text{kHz}$ for SiAl wire with 25 μm diameter, 3mm length and 0.3mm loop height.
- The wire displacement for a given force depends on the fourth power of length and forces in the plane of the wire loop have two orders of magnitude less than where the force is perpendicular to the wire.
- The transient response back e.m.f. method offers a powerful and easy way of identifying the location of bond wires resonant frequencies, even if they are too small to be seen by eye.
- The Q – value for 2.3mm bond wire oscillations was determined experimentally as 137 ± 38 .
- Over-bonded wires appeared to break much more easily than normal wires, but other characteristics of oscillation appeared similar to normal bonds.
- A useful extension to the problem would be to investigate the effect of low amplitude, long term wire oscillations to see if bonds can be broken away from resonance over long periods.
- Through a combination of wire orientations and lengths it appears that the problem has been avoided in ATLAS. The implementation of a VETO against constant frequency triggers would be desirable to further safeguard the experiment.

Section 7 – Bibliography

1. *Wire-Bond Failures Induced by Resonant Vibrations*, Reid Mumford – the investigation into the CDF bond wire problem.
2. *Resonant Bond Wire Problem*, Tony Weidberg – initial experiments to assess the danger of the bond wire problem in ATLAS.
3. *World of Physics*, Eric Weisstein – much of the detail behind the analytical equations can be found here.
4. *RAL Photo Gallery* - for many of the images used of ATLAS components in this report

Section 8 – Appendix

8.1 – Labview Program

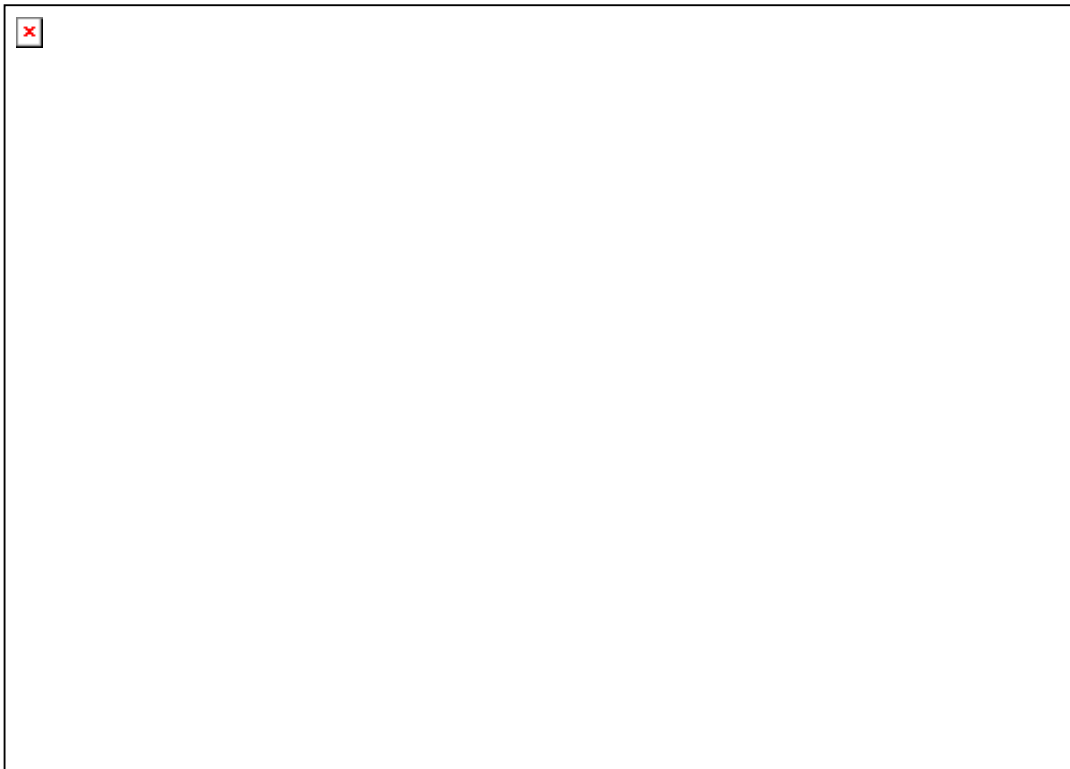
Below is the diagram and front panel for the Labview program used to scan a frequency range and photograph the wire at each step. It also monitored the voltage across the wire using a sample from the oscilloscope. Smaller programs comprising of sections of the code below were also used in the actual experiment to obtain specific frequencies.

stepper II.vi

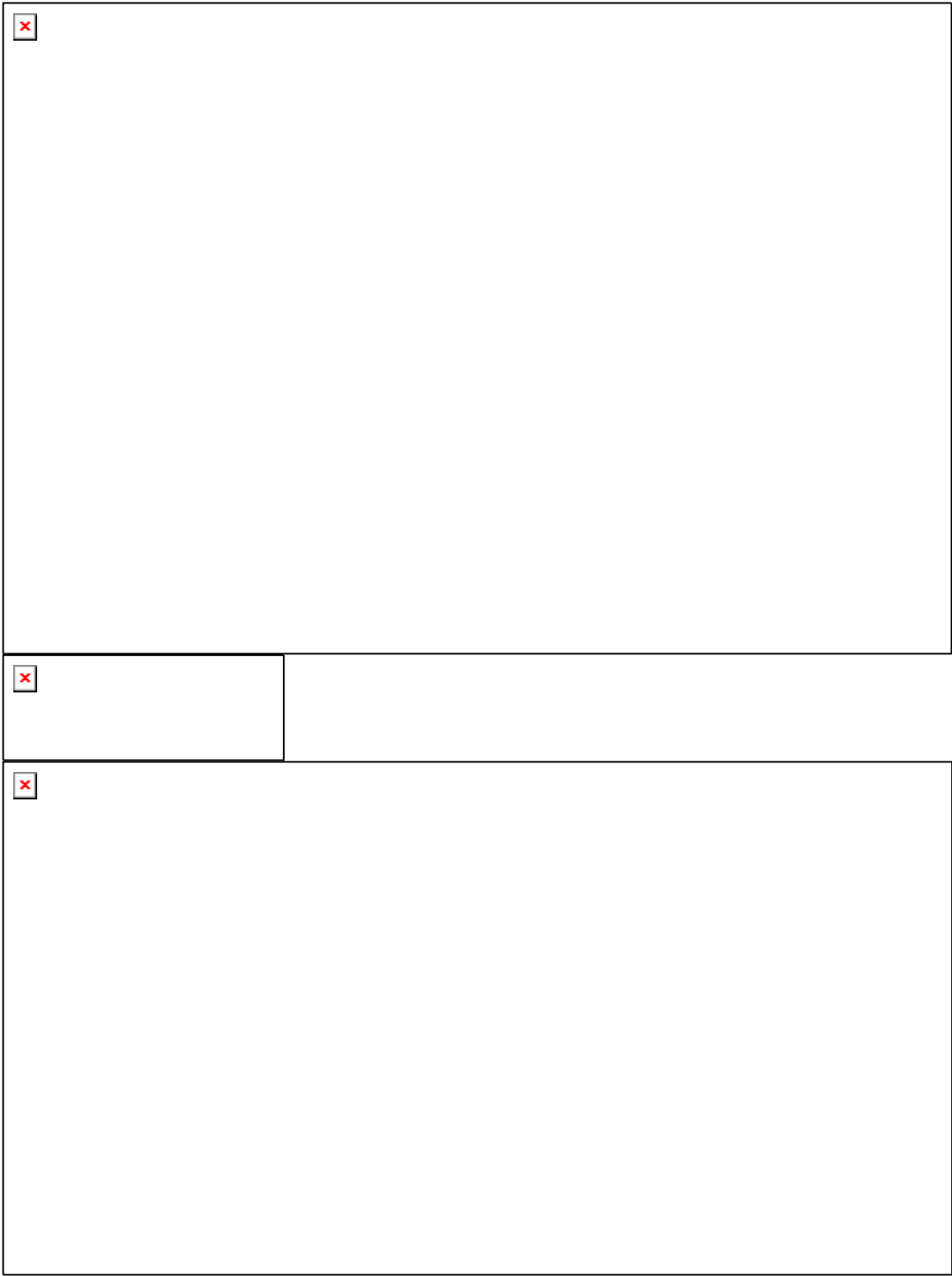
Connector Pane





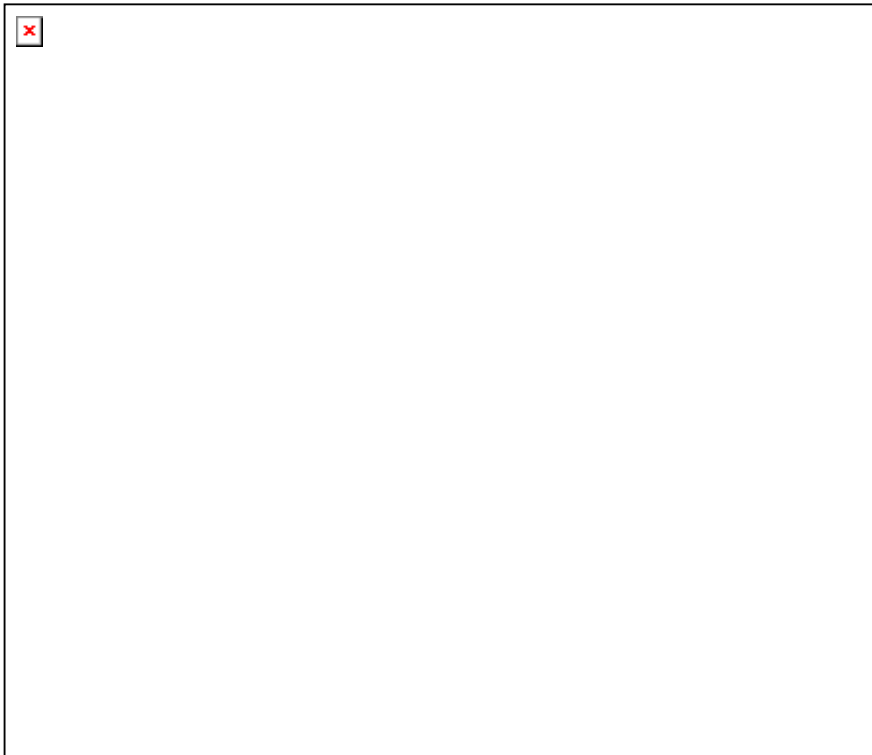
Front Panel

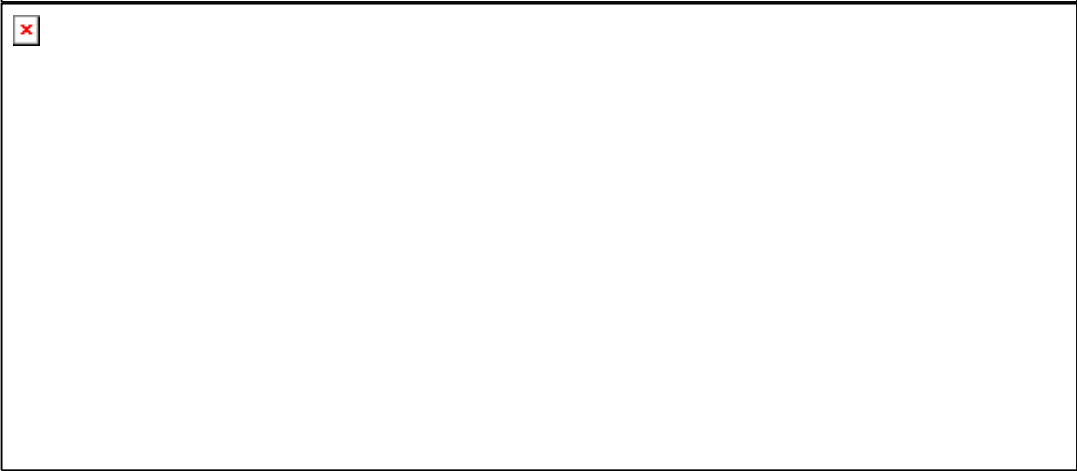
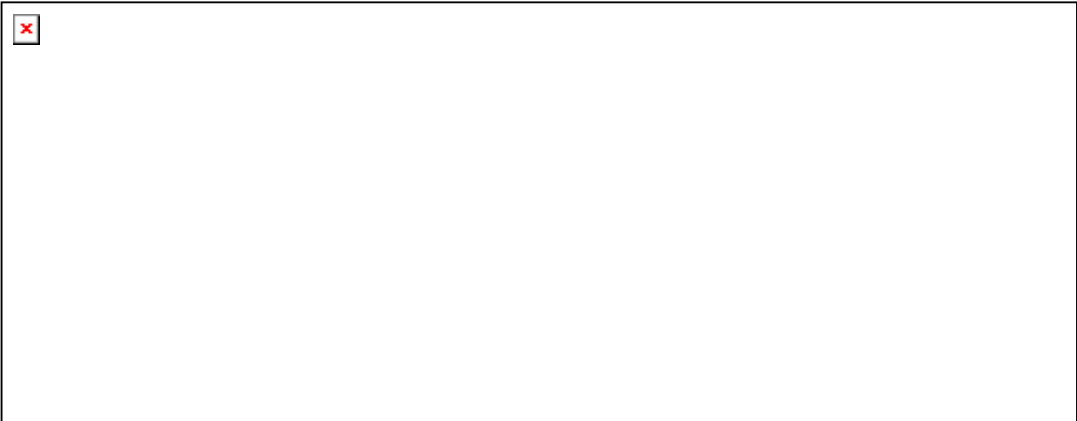


Block Diagram



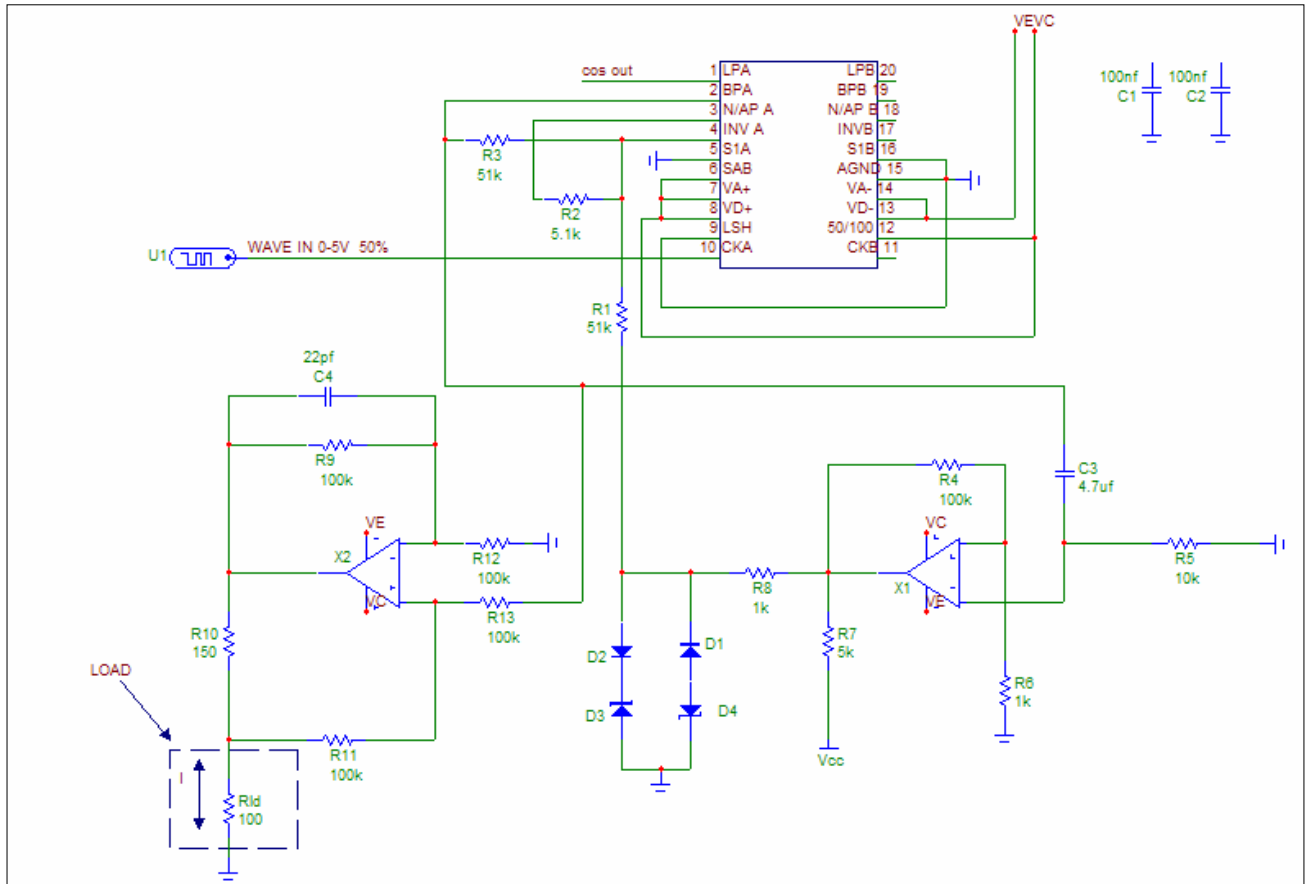
<div data-bbox="245 293 277 327"></div>	
<div data-bbox="245 875 277 909"></div>	





8.2 – Square to Sine Convertor

Shown below is the square to sine convertor and constant current source circuit used in the experiment. Many thanks to Giulio Villani at RAL for designing the circuit and helping with its construction.



The large IC shown above is a second order BP switched capacitor filter, which, together with a comparator (the right op-amp) forms an oscillator at the resonant frequency of the filter. This can be varied by the switching frequency, and so a square wave is transformed to a sinusoidal one. A Howland constant current source (left op-amp) transforms a constant voltage (3V in this case) into a constant current, depending on the value of R10. (using $I = V / R$) The final output signal is given by:

$$I_{out} = \frac{V}{R} * \sin\left(2\pi \frac{f_{in}}{50} t\right)$$